

Combining optical trapping in a microfluidic channel with simultaneous micro-Raman spectroscopy and motion detection

Penelope F. Lawton, Christopher D. Saunter and John M. Girkin
Durham University, South Road, Durham, England DH1 3LE

ABSTRACT

Since their invention by Ashkin optical tweezers have demonstrated their ability and versatility as a non-invasive tool for micromanipulation. One of the most useful additions to the basic optical tweezers system is micro-Raman spectroscopy, which permits highly sensitive analysis of single cells or particles. We report on the development of a dual laser system combining two spatial light modulators to holographically manipulate multiple traps (at 1064nm) whilst undertaking Raman spectroscopy using a 532nm laser. We can thus simultaneously trap multiple particles and record their Raman spectra, without perturbing the trapping system. The dual beam system is built around micro-fluidic channels where crystallisation of calcium carbonate occurs on polymethylmethacrylate (PMMA) beads. The setup is designed to simulate at a microscopic level the reactions that occur on items in a dishwasher, where permanent filming of calcium carbonate on drinking glasses is a problem. Our system allows us to monitor crystal growth on trapped particles in which the Raman spectrum and changes in movement of the bead are recorded. Due to the expected low level of crystallisation on the bead surfaces this allows us to obtain results quickly and with high sensitivity. The long term goal is to study the development of filming on samples in-situ with the microfluidic system acting as a model dishwasher.

Keywords: Optical Tweezers, Raman Spectroscopy, Crystallization, Motion Detection

1. INTRODUCTION AND THEORETICAL CONSIDERATIONS

Since their use by Ashkin in the 1980s¹, optical tweezers have proved themselves to be a highly versatile tool for micromanipulation. Optical tweezers use light tightly focussed through a high numerical aperture microscope objective, which restricts the Brownian motion of particles of the order of microns in diameter to the trapping beam focus. This allows us to perform analysis on microscopic sized objects without attaching them to coverslips, which can pose other problems, or using more invasive procedures. If we wish to investigate these objects non-invasively, a popular method for studying microscopic objects is spectroscopy, where light which has interacted with a sample can be analysed. Combining the two methods of tweezing and spectroscopy allows us to obtain spectra from very small samples without complications arising from its motion. We have developed a system which combines micro-Raman spectroscopy with optical tweezers by using two separate laser beams; one to trap particles at 1064nm and one to excite the Raman emission at 532nm. This has previously been successfully accomplished with beads² and even biological materials³; we intend to use this to investigate chemical adsorption onto trapped species in a microfluidic channel.

Raman spectroscopy was first used in 1928 by Sir C. V. Raman to investigate inelastic scattering of sunlight, using a narrow band photographic filter to create monochromatic light and blocking this light with a crossed filter. He found a small amount of light had changed frequency and passed through the crossed filter. The Raman effect occurs when light impinges on a molecule and interacts with the bonds of that molecule, causing it to be excited. The molecule then relaxes and emits a photon with less energy, and the shift in energy is characterized as the Raman-Stokes shift, $\Delta\omega$. From analysis of the emitted light, we can deduce which bonds are excited in the molecule and thus can identify it by comparing it to previously found Raman spectra, forming

Further author information: (Send correspondence to Penny Lawton)
Penny Lawton.: E-mail: p.f.lawton@durham.ac.uk, Telephone: +441913343727

a spectroscopic molecular fingerprint. In this work we use Raman spectroscopy to investigate the build up of calcium carbonate on microscopic beads. Our motivation for this is the macroscopic crystallization of calcium carbonate in dishwashers on transparent kitchenware, in particular polymethylmethacrylate or PMMA (more commonly known as acrylic). This crystallization manifests as a loss of shine on items cleaned in a dishwasher, undermining their time-saving and energy-efficient benefits. The crystallization is mostly caused by calcium ions in hard water reacting with carbonates in dishwasher detergents that work to cut out grease on dishes, producing calcium carbonate crystals (CaCO_3)⁴. The way in which this build up occurs during the dishwasher cycle is currently not well-characterized. Through flowing a mix of calcium ions and carbonates past an optically trapped micron sized sample of a material commonly washed in a dishwasher, for example polymer microspheres which are commonly available, it is possible to analyse the amount of crystallization which occurs over time through the use of Raman spectroscopy on Calcium Carbonate, which has strong well known Raman peaks common to each crystal polymorph^{5,6}.

Recently microfluidic platforms, which consist of liquid-handling structures of the order of micrometres in cross-section, have become valuable devices in that they use low liquid volumes meaning less waste and a high degree of control over chemical reactions^{7,8}. To give us control over the adsorption reaction we wish to study, we have made use of a microfluidic flow channel in which optical trapping occurs. The rate of flow in a microfluidic channel is determined by the size of the channel and the input flow rate, which is delivered by two syringe pumps. As optical trapping is easier under lower flow rates due to the force of moving fluid the maximum flow rate is limited by the maximum restorative force of the optical trap which limits the speed of the rate of reaction, thus the solutions are heated externally before entering the channel.

We also intend to trap several particles at once through the use of a spatial light modulator⁹. Through the use of spatial light modulators in both the tweezing and Raman beams, it is possible to trap several particles and Raman-excite each in turn, and thus we can study the molecular environment of several trapped species. This will allow us to obtain more of an average, as the beads are unlikely to coat uniformly. While Raman spectroscopy is useful for telling us what is building up on the bead surface, it would also be useful to know how quickly species are building up. This is achieved through the use of a DSI-640 smart camera which is capable of tracking particle position with a built in centroiding algorithm¹⁰. Through tracking a particle's position in an optical trap we can obtain its power spectrum through a fourier transform of the autocorrelation function of the particle's movement^{11,12}. The power spectrum takes the form of a Lorentzian curve, and the corner (or 'knee') frequency of the curve is given by:

$$f_c = \frac{\kappa}{2\pi\gamma_0} \quad (1)$$

where κ is the trap stiffness and γ_0 is the Stokes Drag for a spherical particle, given by $\gamma_0 = 6\pi\rho\nu R$. The trap stiffness is sensitive to the bead environment, particularly its mass and refractive index. We intend to use the corner frequency calculated from measurements of the bead's motion over time while any crystallization takes place as a method of monitoring the crystallization before obtaining micro-Raman spectra.

2. METHODOLOGY

2.1 Apparatus

A bespoke Raman Tweezing setup was built as shown in figure 1. A 1W 1064nm Nd:YAG laser was used for optical trapping. The beam was expanded onto a Holoeye PLUTO spatial light modulator, and then reflected by the dichroic mirror to join the 532nm laser beam. The 532nm laser was a 50mW frequency doubled Nd:YAG laser and was used for excitation of Raman spectra at a power of a few mW at the sample. The beams were steered vertically to overfill the back aperture of a 100x microscope objective with a numerical aperture NA=1.25 (Nikon) using a polychroic mirror (Chroma) designed to reflect both 532nm and 1064nm light and transmit all other wavelengths. $3\mu\text{m}$ diameter PMMA beads (Phosphorex Inc.) were trapped in a thin-bottomed ($145\mu\text{m}$ bottom thickness) microfluidic flow slide (Micronit Microfluidics), as shown in the schematic. The microreactor had a total internal volume of $1\mu\text{L}$ and a channel length of 42mm. Light, back-scattered from the objective,

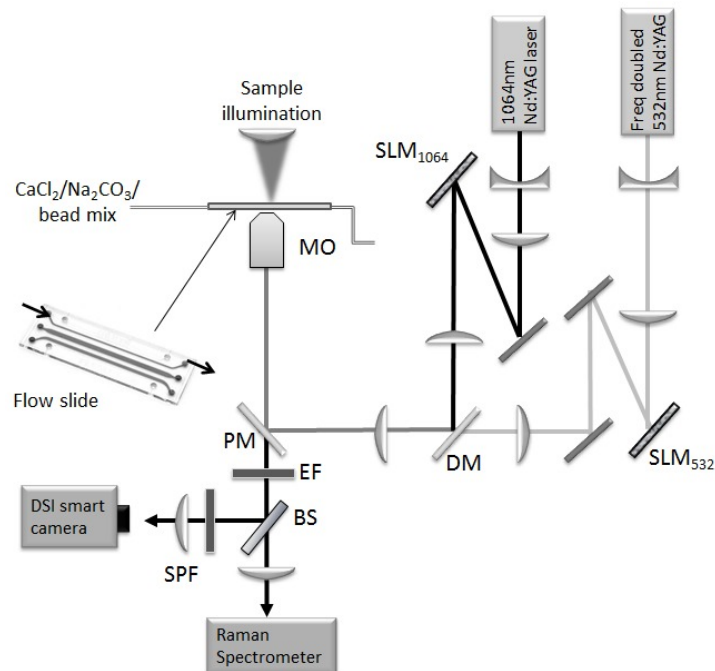


Figure 1. Schematic of the Raman Tweezing setup. PM=polychroic mirror, BS=20:80 beamsplitter, DM=dichroic mirror, MO=microscope objective. Inset: Microfluidic slide image taken from micronit microfluidics

was passed through a 20:80 beamsplitter, where 80% of the light was directed onto a razor-edge longpass filter (Semrock) and was focussed onto a $400\mu\text{m}$ core diameter fibre coupled to the spectrometer. The spectrometer used was a USB2000+ spectrometer from OceanOptics. The smaller percentage of the back scattered light was passed through a 532nm long pass filter and a 1064nm short pass filter to block the laser light but allow the imaging light to be focussed onto the DSI-640 smart camera by Durham Smart Imaging. This is capable of acquiring object positions at very high frame rates for small selected regions (100×100 pixels for example gives a frame rate of 5000Hz).

2.2 Experimental technique

To check whether crystallization would occur on the beads, samples of beads were mixed on a stirring hotplate at 50°C with a 2.75mM solution of calcium chloride and 18mM sodium carbonate and viewed under a microscope after set periods of time, as shown in figure 2. After 10 minutes there is no crystallization, but after 30 minutes there are clear seeds forming, with larger crystals of amorphous calcium carbonate forming within 1 hour and large calcite crystals forming after 90 minutes. This suggests that the crystallization begins somewhere between 30 minutes and 1 hour of constant stirring and heating. It is also of note that not all beads are coated homogeneously. Adding a surfactant and sonicating the solution appears to increase the number of beads which are coated. Under controlled conditions with a constant flow rate and a trapped bead the coating was expected to be fairly consistent over time.

Reactions and optical trapping were carried out in a microfluidic channel with a cross section of $500\mu\text{m}$ by $50\mu\text{m}$. The inlet was connected to two syringe pumps (New Era NE-300) and the tubing (PFA) was externally heated through use of a hot plate heated to 60°C . A thermocouple gave the temperature at the microfluidic slide as 50°C . Sample solutions of 4mL 2.75mM calcium chloride and 4mL 18mM sodium carbonate were mixed briefly with $40\mu\text{L}$ of $3\mu\text{m}$ diameter polymethylmethacrylate beads (Phosphorex) and 10mL of surfactant. These concentrations were used as they gave good crystallization on macroscopic PMMA films on silicon. A second

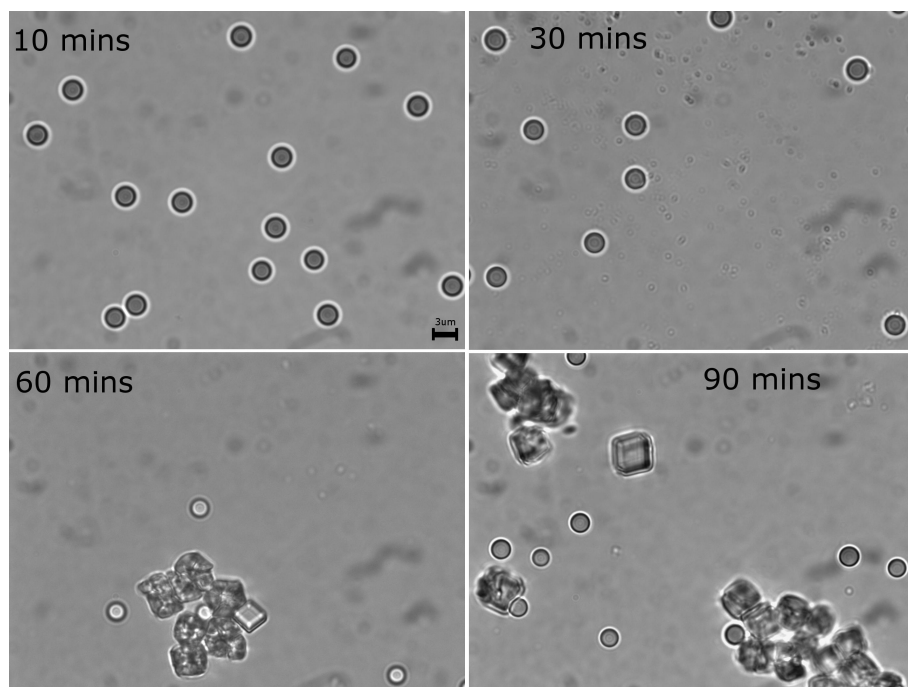


Figure 2. Confocal microscope images of PMMA beads at 100x magnification showing development of calcium carbonate crystals around beads after different lengths of time. Beads are 3 microns in diameter

solution of 4mL calcium chloride and 4mL sodium carbonate was also mixed. The syringe pumps were set to flow each solution through the channel at a total flow rate of 0.5mL/hour and the flow rate was decreased through the use of a second piece of connected tubing acting as a hydraulic resistor to reduce the total flow rate in the channel to 0.02mL/hour, corresponding to a Reynolds number in the channel of 0.04. This was necessary as the internal mechanism of the syringe pumps caused a disturbing amount of flow oscillations when used at low flow speeds which was not present at higher flow speeds. The flow was shown to be consistent through the channel by the use of fluorescent tracker beads and particle image velocimetry calculations. Beads were trapped in the channel during the flow of solution and a region selected on the camera which gave a frequency of 1300Hz; the beads were known to have a corner frequency far below this from calibrations. Particle position readings were then taken for 60 seconds with a spacing of 30 seconds. As the fluid flow caused the x-direction motion of the beads to be somewhat erratic, only the y-direction motion was considered during power spectrum calculations. Raman spectra were also taken of the trapped PMMA beads with an integration time of 30 seconds.

3. RESULTS AND DISCUSSION

3.1 Raman Spectra

Figure 3 shows the Raman spectra of toluene and PMMA. Toluene has a strong Raman spectrum and is typically used to calibrate Raman spectrometers; as can be seen, our device has the characteristic peaks at 786cm^{-1} , 1003cm^{-1} (aromatic ring chain), 2940cm^{-1} and 3057cm^{-1} (C-H stretching). PMMA is one of the main background spectra aside from glass that need to be subtracted from the overall spectrum, and we are able to detect the main peaks at 1460cm^{-1} , 1736cm^{-1} and 2957cm^{-1} (again indicative of C-H stretching). Figure 4 show the Raman signal after background subtraction of calcium carbonate formed on the coverslide from the solutions made in section 2.2. The peak at 1085cm^{-1} is clear, indicating the presence of the carbonate (CO_3) ion. From this we demonstrate that our system is capable of taking Raman spectra of trapped species.

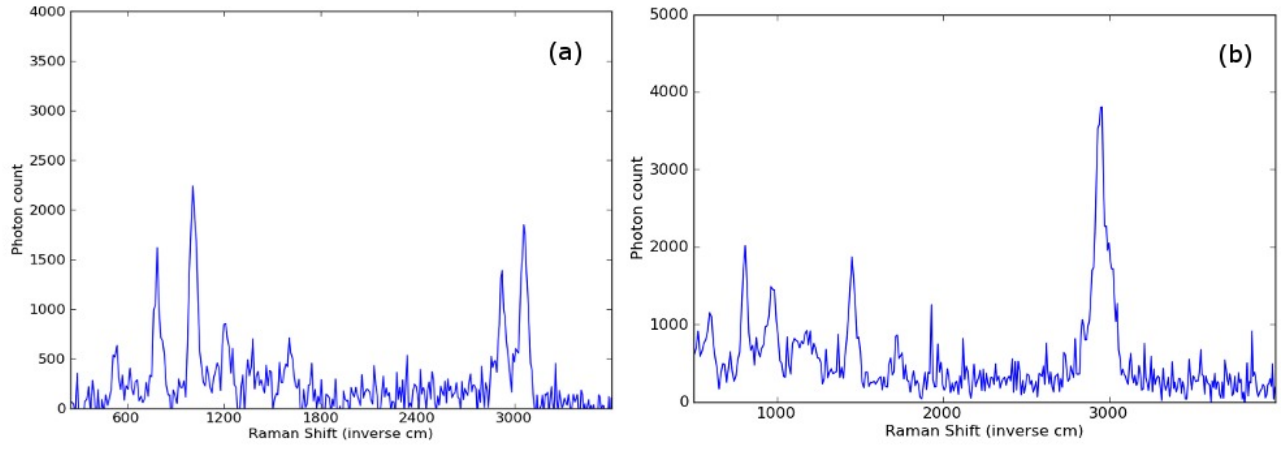


Figure 3. Raman spectra of (a) toluene (used for Raman spectrometer calibration) and (b) a single trapped PMMA bead

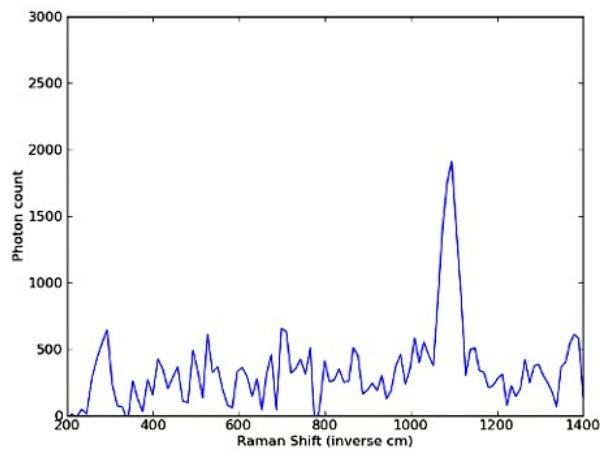


Figure 4. Raman spectrum of calcium carbonate formed on a cover slide

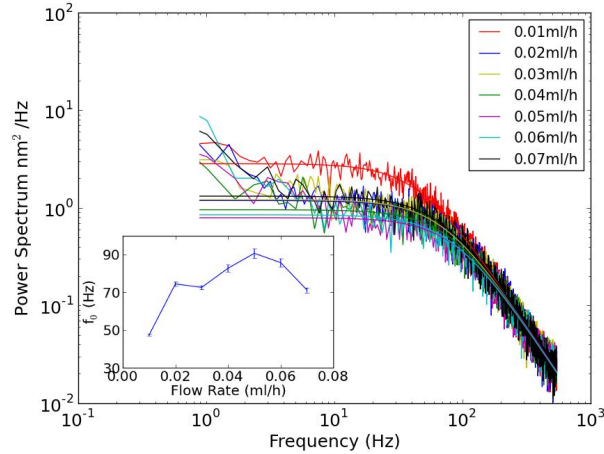


Figure 5. Temporal power spectra for a $3\mu\text{m}$ PMMA bead trapped in distilled water 0.6W with distilled water flowing past at different flow rates. Inset: Showing the change of 'corner frequency' with flow rate

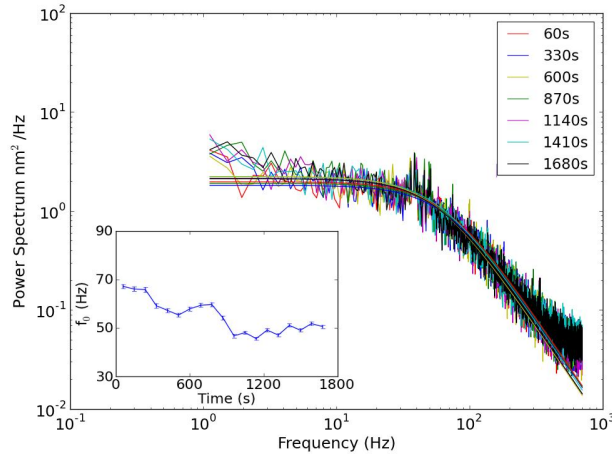


Figure 6. Power spectra for a $3\mu\text{m}$ PMMA bead over time trapped in distilled water flowing at 0.02ml/h at 0.6W . Inset: Calculated corner frequency from Lorentzian fit over time

3.2 Position detection calibrations

The system was calibrated to test the response of the tracking algorithm in the camera when different syringe pump flow rates were used to pump a plain medium (distilled water) past a trapped $3\mu\text{m}$ diameter bead. From figure 5, the corner frequency appears to increase at higher flow rates. This may be due to the fluid flow causing the bead to be slightly pushed to a certain point in the potential 'well' of the optical trap, thus somewhat stabilising its movement.

The response of the system was also tested while plain distilled water was flown past a trapped bead over time as a control, as demonstrated in figure 6. It was found that the corner frequency is roughly stable over time, although there are some small fluctuations, which we would expect due to the random nature of the Brownian motion of the bead in the trap.

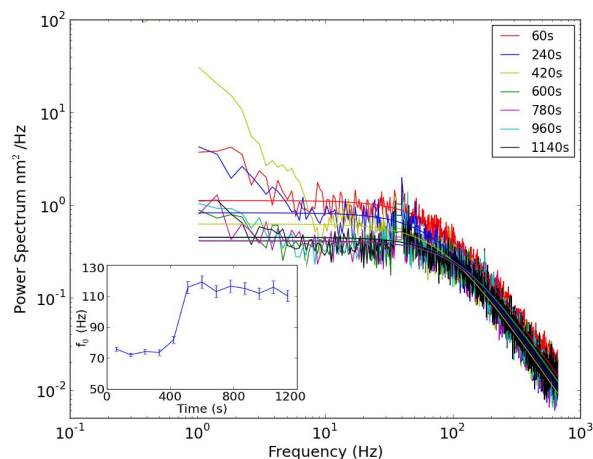


Figure 7. Power spectra over time for a $3\mu\text{m}$ PMMA bead trapped in a mixture of CaCl_2 and Na_2CO_3 pumped at a flow rate of 0.02ml/h . Inset: Calculated corner frequency from Lorentzian fit over time

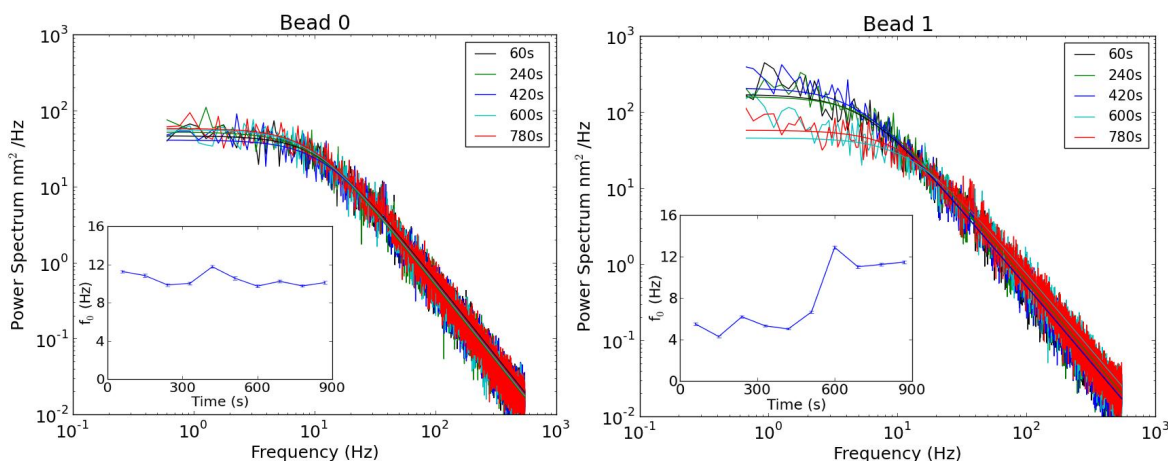


Figure 8. Power spectra for two holographically trapped $3\mu\text{m}$ PMMA beads in a mixture of CaCl_2 and Na_2CO_3 pumped at a flow rate of 0.02ml/h . Inset: Calculated corner frequency from Lorentzian fit over time

3.3 Power spectra with solution present

From figure 7 we can see there is a change in the power spectrum over time as the corner frequency increases rapidly after 500 seconds of continuous fluid flow past the bead, indicating that at this point crystallisation has occurred on the bead surface. There is a spike in the spectrum between 30 and 40Hz, which was thought to be due to vibrations of pipes leading from the syringe pumps due to mechanical oscillations; while this does not have a substantial effect on the Lorentzian fit it could be eliminated by using an alternative method of fluid flow. The power spectrum of the 'tail' of the plot also increases, which indicates a change in the bead's intrinsic Brownian motion due to the buildup.

It is important to note that the change in corner frequency over time does not indicate a change in trap stiffness but rather a perturbation of the laser spot trapping the bead, at which point equation 1 may no longer be valid. Increasing the bead volume tends to increase the corner frequency due to both the increase in viscous drag and the dependency of trap stiffness on volume, which for Mie particle is non-linear.¹³ This change was not always noted because beads were not always coated, as expected from previous attempts to coat the beads on stirring hot plates. To increase the chance in seeing a change in the trap stiffness, it is helpful to trap more than one bead. An example of this may be seen in figure 8. While one bead has not been coated, the other one shows a

clear change in corner frequency over time, indicating a buildup. It is important to note however that since the power is now shared between traps the corner frequencies are generally lower as the trap stiffness as a whole has decreased due to less light in the traps. While there is not enough information to deduce the mass of buildup from changes in the corner frequency of the power spectrum, as the inertial term containing the mass drops out of the Langevin equation when we undertake the power spectrum calculation, this nevertheless provides us with a powerful tool for deducing when there is buildup on a bead. It is possible to increase the time resolution of this by decreasing the time over which position measurements are taken, although this introduces more error during Lorentzian fitting to the power spectra.

3.4 Further work

Calcium carbonate formation on PMMA beads is clearly hard to control, but we are able to detect if something begins to build up on a bead through close monitoring of the bead's movement. Beads that are already coated tend to attract more buildup, and so one way to monitor buildup would be to coat a bead with calcium carbonate, flow distilled water past the bead then flow the calcium chloride and sodium carbonate mixture past the bead again.

While it may not be possible to deduce the mass of calcium carbonate building up on a bead from monitoring its position in an optical trap, it may be deduced by comparison of the height of the peaks in the Raman spectrum. Use of a dedicated Raman spectrometer allows faster acquisition times due to lower noise and a higher resolution spectrum to pinpoint the peak position, thus simultaneous measurements with the power spectra may be taken

Given that calcium carbonate is a birefringent material, once there is buildup, it is possible to rotate coated beads using elliptically polarised light¹⁴ and from changes in the speed of this rotation an alternative method of monitoring the mass of the buildup is possible.

ACKNOWLEDGMENTS

This work was funded by the UK Government Regional Development Fund. The authors would also like to thank the SMC³ team for their support and expertise.

REFERENCES

- [1] Ashkin, A., Dziedzic, J. M., Bjorkholm, J. E., and Chu, S., "Observation of a single-beam gradient force optical trap for dielectric particles," *Opt. Lett.* **11**, 288–290 (1986).
- [2] Creely, C., Singh, G., and Petrov, D., "Dual wavelength optical tweezers for confocal Raman spectroscopy," *Opt. Comm.* **245**, 465–470 (2005).
- [3] Bankapur, A., Zachariah, E., Chidangil, S., Valiathan, M., and Mathur, D., "Raman tweezers spectroscopy of live, single red and white blood cells," *PLoS ONE* **5**, e10427 (2010).
- [4] Wiechers, H., Sturrock, P., and Marais, G., "Calcium carbonate crystallization kinetics," *Water Res.* **9**, 835–845 (1975).
- [5] Unvros, J., Sharma, S., and MacKenzie, F., "Characterization of some biogenic carbonates with Raman spectroscopy," *Am. Mineral.* **76**, 641–646 (1991).
- [6] White, S., "Laser Raman spectroscopy as a technique for identification of seafloor hydrothermal and cold seep minerals," *Chem. Geol.* **259**, 240–252 (2009).
- [7] Capretto, L., Cheng, W., Hill, M., and Zhang, "Micromixing within microfluidic devices," *Top. Curr. Chem.* **304**, 27–68 (2011).
- [8] DeMello, A., "Control and detection of chemical reactions in microfluidic systems.," *Nature* **442**, 394–402 (2006).
- [9] Ferrari, E., Cojoc, D., Emiliani, V., Garbin, V., Moisan, M. C., and Fabrizio, E. D., "Three-dimensional holographic optical tweezers implemented on spatial light modulator," *Proc. SPIE* **5972**, 17–22 (2005).
- [10] Silburn, S., Saunter, C., Girkin, J., and Love, G., "Multidepth, multiparticle tracking for active microrheology using a smart camera," *Rev. Sci. Instrum.* **82**, 033712 (2011).

- [11] Gibson, G., Leach, J., Keen, S., Wright, A., and Padgett, M., “Measuring the accuracy of particle position and force in optical tweezers using high-speed video microscopy,” *Opt. Express* **16**, 405–412 (2008).
- [12] Berg-Sørensen, K. and Flyvbjerg, H., “Power spectrum analysis for optical tweezers,” *Rev. Sci. Instrum.* **75**, 594–612 (2004).
- [13] Bormuth, V., Jannasch, A., Ander, M., van Kats, C., van Blaaderen, A., Howard, J., and Schäffer, E., “Optical trapping of coated microspheres,” *Opt. Express* **16**, 13831–13844 (2008).
- [14] Eriksen, R. L., Rodrigo, P. J., Daria, V. R., and Glückstad, J., “Spatial light modulator–controlled alignment and spinning of birefringent particles optically trapped in an array,” *Appl. Opt.* **42**, 5107–5111 (2003).